Pramana – J. Phys. (2022) 96:134
https://doi.org/10.1007/s12043-022-02379-y

Stabilisation of higher-order solitons by the compensation of quintic nonlinearity, fourth-order dispersion and intrapulse Raman scattering in optical fibres

MOUSSA SMADI

Laboratoire de Physique des Rayonnements et de leurs Interactions avec la Matière (LPRIM), Département de Physique, Faculté des Sciences de la Matière, Université de Batna 1, Hadj Lakhdar, Allées 19 Mai, Route de Biskra, 05000 Batna, Algeria
E-mail: msmadi@univ-batna.dz

MS received 22 May 2021; revised 22 February 2022; accepted 28 February 2022

Abstract. The propagation of a higher-order soliton in an ideal single-mode optical fibre under higher-order dispersion and higher-order nonlinearity is much affected by quintic nonlinearity, fourth-order dispersion and intrapulse Raman scattering. We use a compact split-step Padé scheme to numerically study the stabilisation of higher-order solitons by these effects in optical fibres. Our results show that the relative amplitudes of these two dispersive sideband waves, which originate from the fourth-order dispersion decrease or even eliminated by the increasing values of quintic nonlinear coefficient, in the presence of the intrapulse Raman scattering, and the higher-order soliton returns almost to its original shape.

Keywords. Higher-order solitons; fourth-order dispersion; quintic nonlinearity; intrapulse Raman scattering.

PACS Nos 42.65.Tg; 42.65.Jx; 42.81.Dp

1. Introduction

It is well known that, under ideal circumstances, fundamental soliton pulses can travel for long distances in optical fibres without noticeable deformations [1,2]. In addition, the propagation without any distortion of higher-order optical soliton stops the presence of higher-order dispersive effects. Typically, a higher-order soliton decays into its constituent fundamental solitons in the presence of such perturbations, a phenomenon referred to as the soliton fission [3,4]. After fission, higher-order dispersive impacts transmit a quantity of the pulse energy in the form of a dispersive wave at a specific frequency set by the phase matching condition [5,6]. The emission of the non-solitonic radiation (NSR) in the form of a dispersive wave is of particular importance for supercontinuum generation [4–6]. Numerical simulation indicates that a value of τ_R as small as 10^{-3} can induce fission of higher-order solitons [7]. It was noted that, the fourth-order dispersion gives rise to two NSR peaks on the red and blue sides of the original pulse spectrum [8]. However, optical fibres present higher-order nonlinear and dispersion effects that can alter the stability of very short and ultra-intense solitons, especially with the interplay of higher-order dispersion effects such as third-order dispersion (TOD) or fourth-order dispersion (FOD). Nonlinear effects represent the main source of limitation of the rate of data transferred through an optical fibre. Quintic nonlinearity, the most important nonlinear effect, is due to the saturation of optical field [9]. It was indicated that, the quintic nonlinearity coefficient, with a value of $1\,\mathrm{W}^{-2}/\mathrm{km}$, will result in a significant transmission impairment, and Q factor of the transmission system is reduced by 1.9 at a distance of 120 km. When the optical transmitter power increases from 0.01 W to 0.5 W, the average Q factor is decreased by 32.5 [10]. Therefore, the impact of this parameter must be taken into consideration in the study of ultra-intense optical solitons. In this study, we investigate numerically the combined influence of FOD, quintic effect and intrapulse Raman scattering (IPRS) on the transmission of higher-order solitons in optical fibres.

Published online: 07 July 2022

2. Theoretical model

The propagation of ultra-short and ultra-intense optical solitons in single-mode optical fibre under both higher-order dispersion and higher-order nonlinear effects (such as self-steepening, quintic nonlinearity and intrapulse Raman scattering) can be governed by the generalised Schrödinger equation (GSE), given as follows [1]:

$$\frac{\partial A(Z,T)}{\partial Z} = -\frac{\alpha}{2}A + i\sum_{n=2}^{n=4}\frac{i^n}{n!}\beta_n\frac{\partial^n A}{\partial T^n} + i\gamma\left[|A|^2A + \gamma'|A|^4A + \frac{i}{\omega_0}\frac{\partial}{\partial T}(|A|^2A) - T_R A\frac{\partial|A|^2}{\partial T}\right], \quad (1)$$

where $i = \sqrt{-1}$, $A(Z,T)$ represents the amplitude of the field envelope of the optical soliton, $T = t_{\text{lab}} - Z/v_g$ is the temporal coordinate measured in a frame of reference moving with the soliton at the group velocity v_g, Z is the spatial coordinate representing the distance the pulse passes and β_2, β_3, β_4 represent dispersion parameters of the second, third and fourth orders. α is the fibre loss coefficient. $\gamma = n_2\omega_0/cA_{\text{eff}}$ and γ' are respectively the nonlinear Kerr effect and the quintic nonlinear coefficients. n_2 is the nonlinear index coefficient, and for silica fibres, $n_2 = 2.2\times10^{-20}\,\text{m}^2/\text{W}$ at the wavelength $\lambda \sim 1.55\,\mu\text{m}$ [1]. The term proportional to $1/\omega_0$ governs the Kerr dispersion that is responsible for self-steepening (SS) phenomenon arises from the intensity dependence of group velocity and it creates an optical shock on the trailing edge of the pulse in the absence of group velocity dispersion [11]. The last term is responsible for the self-frequency shift induced by IPRS and T_R is related to the Raman response function. At wavelength $\lambda_p \sim 1.55\,\mu\text{m}$, $T_R \approx 3\,\text{fs}$ [1].

3. Numerical scheme

First, we proceed to normalise model equation (1), by choosing new variables as follows:

$$t = \frac{T}{T_0},\ z = \frac{Z}{L_D},\ L_D = \frac{T_0^2}{|\beta_2|},\ L_D' = \frac{T_0^3}{|\beta_3|},\ L_D'' = \frac{T_0^4}{|\beta_4|},$$
$$L_{NL} = \frac{1}{\gamma P_0},\ \kappa = \frac{1}{\gamma' P_0^3},\ s = \frac{1}{\omega_0 T_0},\ \tau_R = \frac{T_R}{T_0},$$

and

$$u(z,t) = \frac{A(z,t)}{\sqrt{P_0}},$$

where T_0 is the initial pulse width, L_D, L_D', L_D'' and L_{NL} are respectively the dispersion lengths for different orders and nonlinear length. The parameters s and τ_R govern the impacts of SS and IPRS respectively. Both these effects are quite small for picosecond pulses but must be taken into consideration for ultra-short pulses with $T_0 < 0.1\,\text{ps}$ [1]. It is well known that one of the main causes of signal degradation in long-distance fibre-optic communication systems is the fibre loss. However, the fibre loss problem was solved prior to 1991, firstly, by using repeaters periodically installed in the transmission line. A repeaterless soliton transmission system using distributed Raman gain provided by the fibre itself to compensate for the fibre loss was suggested by Hasegawa [12] in 1983. Finally, the concept of all-optical transmission using the distributed Raman amplification was replaced by lumped amplification during the 1990s, using erbium-doped fibre amplifiers (EDFAs). Using lumped EDFAs, the amplification occurs over a very short distance ($\sim 10\,\text{m}$), which compensates for the loss occurring over 40–50 km [13]. Based on these realistic data obtained from fibre-optic communication systems, we can numerically omit the attenuation coefficient ($\alpha = 0$). Equation (1) can be written after normalisation as follows:

$$\frac{\partial u}{\partial z} = -i\frac{\text{sgn}(\beta_2)}{2}\frac{\partial^2 u}{\partial t^2} + \frac{\text{sgn}(\beta_3)}{6}\frac{L_D}{L_D'}\frac{\partial^3 u}{\partial t^3} + i\frac{\text{sgn}(\beta_4)}{24}\frac{L_D}{L_D''}\frac{\partial^4 u}{\partial t^4} + i\frac{L_D}{L_{NL}}\left[|u|^2u + \kappa|u|^4u + i\,s\frac{\partial}{\partial t}(|u|^2u) - \tau_R u\frac{\partial|u|^2}{\partial t}\right]. \quad (2)$$

The more convenient form of eq. (2) for the simulation is the new form given as follows:

$$\frac{\partial u}{\partial z} = i\alpha_2\frac{\partial^2 u}{\partial t^2} + \alpha_3\frac{\partial^3 u}{\partial t^3} + i\alpha_4\frac{\partial^4 u}{\partial t^4} + i\left[\alpha_5|u|^2u + \alpha_6|u|^4u - i\alpha_7\frac{\partial}{\partial t}(|u|^2u) + \alpha_8 u\frac{\partial|u|^2}{\partial t}\right], \quad (3)$$

where

$$\alpha_2 = -\frac{\mathrm{sgn}(\beta_2)}{2}, \quad \alpha_3 = \frac{\mathrm{sgn}(\beta_3)}{6}\frac{L_\mathrm{D}}{L'_\mathrm{D}},$$
$$\alpha_4 = \frac{\mathrm{sgn}(\beta_4)}{24}\frac{L_\mathrm{D}}{L''_\mathrm{D}}, \quad \alpha_5 = \frac{L_\mathrm{D}}{L_\mathrm{NL}},$$
$$\alpha_6 = \frac{L_\mathrm{D}}{L_\mathrm{NL}}\kappa, \quad \alpha_7 = -s\frac{L_\mathrm{D}}{L_\mathrm{NL}},$$

and

$$\alpha_8 = -\tau_R \frac{L_\mathrm{D}}{L_\mathrm{NL}}.$$

Equation (3) can be written formally in the form:

$$\frac{\partial u}{\partial z} = \left(\hat{L} + \hat{N}\right) u,$$

where

$$\hat{L} = i\,\alpha_2 \frac{\partial^2}{\partial t^2} + i\,\alpha_3 \frac{\partial^3}{\partial t^3} + i\,\alpha_4 \frac{\partial^4}{\partial t^4},$$
$$\hat{N} = i\,\alpha_5 |u|^2 u + i\,\alpha_6 |u|^4 u + \alpha_7 \frac{\partial}{\partial t}(|u|^2 u) + i\,\alpha_8\, u \frac{\partial |u|^2}{\partial t}.$$

Here, $\hat{L}$ is a linear operator that accounts for all the linear effects and $\hat{N}$ is a nonlinear operator that governs the effect of all the fibre nonlinearities. The approximate solution of eq. (3) is obtained by first solving, for the half step size $\Delta z/2$, the purely linear equation

$$\frac{\partial u}{\partial z} = \hat{L}\, u$$

and then solving the purely nonlinear equation

$$\frac{\partial u}{\partial z} = \hat{N}\, u.$$

The solution of one subproblem is employed as an initial condition for the next subproblem. The validity of this approximation is discussed in ref. [1] using the Baker–Hausdorff formula. The linear equation is solved using the compact Padé scheme algorithm, an implicit scheme that is unconditionally stable and well adapted for the different derivative orders whereas the nonlinear equation is solved using the fourth-order Runge–Kutta scheme (RK4) that satisfies the CFL condition. This scheme is more efficient, rapid and takes less memory space. It is also well adapted to the higher-order derivatives. For more details, see [14,15]. Finally, in our numerical simulation, we assume the following form of initial condition $u(0,t) = N\cosh(t)$, where N represents the order of the soliton and the numerical values of the parameters are given in table 1.

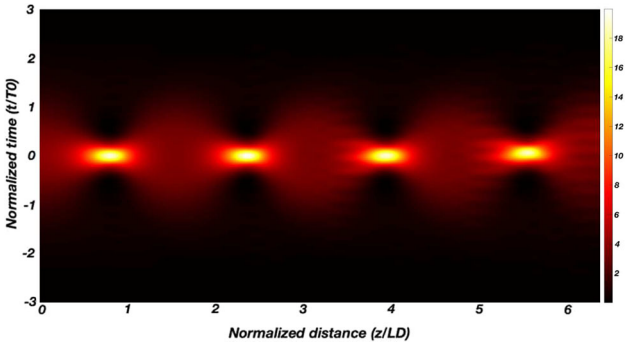

Figure 1. Propagation map of the second-order soliton over six normalised distances.

4. Role of higher-order nonlinear effects

In this paper, we use the numerical solution of the GSE [14], to study the stabilisation of higher-order solitons by the compensation of quintic nonlinearity, fourth-order dispersion and intrapulse Raman scattering in optical single mode fibre. The emission of non-solitonic radiation (NSR), also named Cherenkov wave, by higher-order soliton was first predicted by Akhmediev and Karlsson [8] in an ideal single-mode optical fibre in the presence of group velocity dispersion (GVD), self-phase modulation (SPM) and only the fourth-order dispersion. Further findings were then obtained by many scientists through the split-step Fourier method [1,4]. The symmetry of the red and blue peaks from the centre of the initial soliton is due to the fourth-order dispersion [4,8]. We also know that the amplitude of the radiation peak increases with both the value of third-order dispersion and the soliton order N [16]. In addition, the effect of IPRS on the output spectrum in the presence of FOD alone ($\alpha_3 = 0$), as one may expect, makes the spectrum asymmetric because of a continuous transfer of energy from high frequencies (blue peak) to low frequencies (red peak) [4,17]. On the other hand, we remark that, the periodic amplification of the amplitude of second-order soliton vs. propagation distance is also due to the fourth-order dispersion (see figure 1).

For the propagation of ultrashort and ultra-intense solitons in optical fibres, the Raman contribution to the effective refractive index reduces for soliton widths less than ~ 100 fs, and we know that, this contribution not only reduces but becomes negative, for pulse widths less than ~ 30 fs [18]. This value is the more realistic value for this coefficient, and this justifies our choice of the value $\alpha_8 = -0.04$ in our simulations. For the higher-order nonlinearity, the self-steepening effect plays an essential role. Hence, under the influence of positive SS effect, the peak of the soliton shifts toward the trailing side and the spectrum shifts toward the red side. Hence,

Table 1. Set of parameters used in numerical simulations.

Parameter	α_2	α_3	α_4	α_5	$\lvert\alpha_6\rvert$	α_7	$\lvert\alpha_8\rvert$	Δz	Δt
Value	0.5	0	0.001	1	[0.01 : 0.10]	0	0.04	4.10^{-3}	1/32

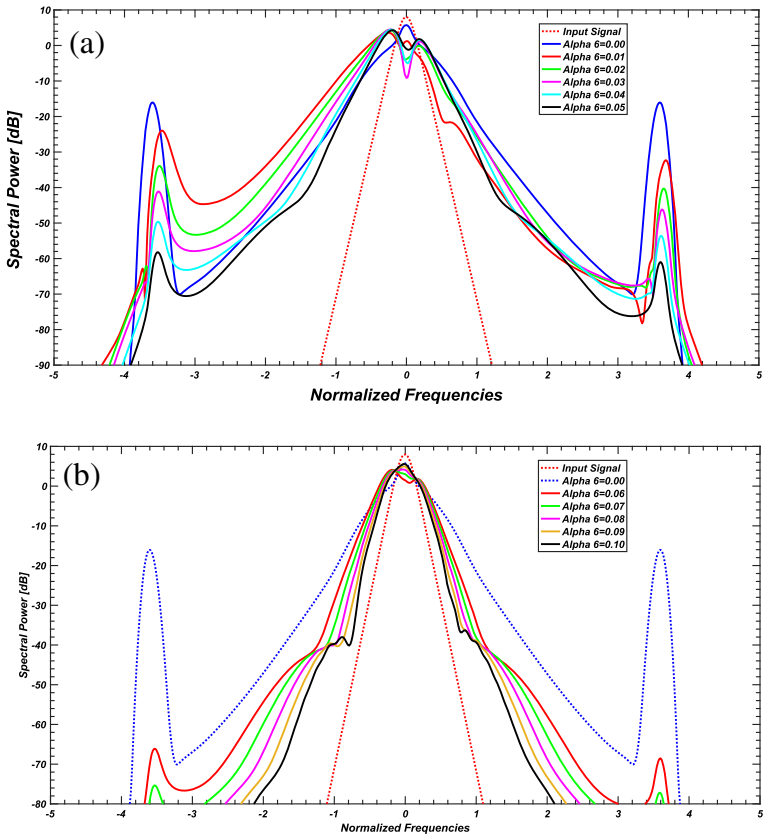

Figure 2. Output spectra evolution function of quintic nonlinear coefficient in the optical fibre when (**a**) $\alpha_6 = [0.01 : 0.05]$, $\alpha_4 = 0.001$, $|\alpha_8| = 0.04$, $N = 2$ and (**b**) $\alpha_6 = [0.06 : 0.10]$, $\alpha_4 = 0.001$, $|\alpha_8| = 0.04$, $N = 2$.

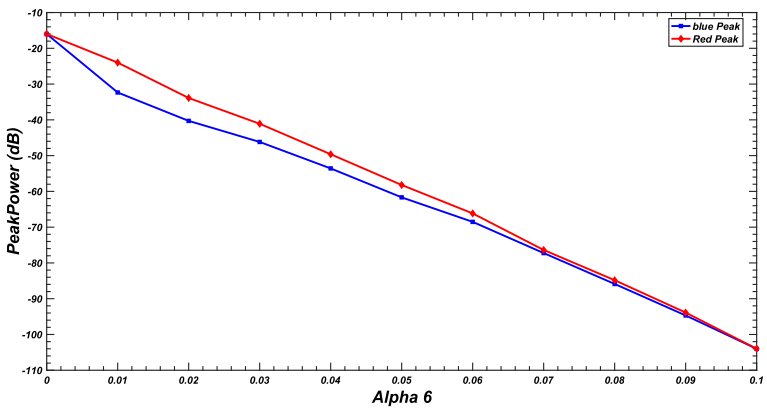

Figure 3. Peaks power vs. the quintic nonlinear coefficient in the optical fibre when $|\alpha_6| = [0.01 : 0.10]$, $\alpha_4 = 0.001$, $|\alpha_8| = 0.04$.

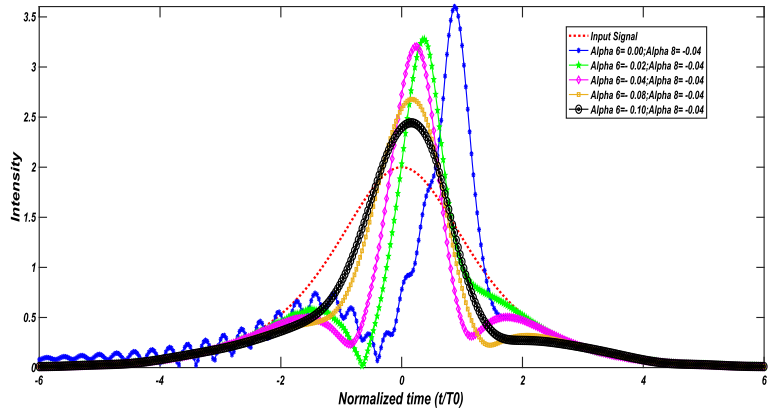

Figure 4. Temporal evolution function of quintic nonlinear coefficient in the optical fibre in the presence of both fourth-order dispersion and intrapulse Raman scattering for $z/L_{\mathrm{D}} = 1.06$ when $|\alpha_6| = [0.00 : 0.02 : 0.10]$, $\alpha_4 = 0.001$, $|\alpha_8| = 0.04$, $N = 2$.

the peak of the soliton shifts toward the leading side of the pulse and the spectrum shifts toward the blue side when the SS effect is negative [19]. By applying the quintic nonlinearity defined by the term α_6 in eq. (3), and the set of coefficients in table 1, the choice of these set values of coefficients depends essentially on the constraints of existence and constancy of the soliton. The first condition asserts that the quintic nonlinearity coefficient must satisfy $\alpha_6 < 0$ in the anomalous dispersion regime, and the other condition comes from the balance of nonlinear effects. For Kerr cubic nonlinearity $\alpha_5 = 1$ will imply that $\alpha_6 < 0$ in the anomalous GVD regime, and thus the cubic and quintic effects may saturate and favours the presence of soliton [20]. In the following discussion, we take into consideration the presence of GVD and SFM with the values indicated in table 1.

We show in figures 2a and 2b the evolution of the output spectrum in the optical fibre as a function of the quintic nonlinear coefficient α_6 in the presence of both the fourth-order dispersion and Raman scattering. As one may expect, the relative positions of both symmetric peaks are not affected by all the values of the quintic nonlinear coefficient, and the solitons radiate at both frequencies $\pm 1/\sqrt{2\,\alpha_8}$, that is in good accordance with the prediction in [8]. However, note that the amplitudes of both peaks are much affected or even more eliminated by the increasing values of quintic nonlinear coefficient. This feature indicates that the dispersive waves transfer energy to the target soliton.

In figure 3 we show the decreasing peak power with increasing values of quintic nonlinear coefficient. Figure 4 represents the temporal variation of the soliton as a function of the increase in the values of the quintic coefficient (α_6), in the presence of the fourth-order dispersion and intrapulse Raman scattering over a distance greater than a soliton period. We first see the amplification of the amplitude of the soliton due to the FOD, and the birth of the ripples at the tail of the soliton as well as the displacement of the peak to the right. These ripples, displacements and amplifications disappear as the value of α_6 increases, and consequently the symmetry of the soliton is restored taking the initial form of hyperbolic secant.

Figures 5a and 5b show the three-dimensional plots of the evolution of higher-order soliton and they represent a comparison between a pulse launched in a single-mode fibre under the unique influence of the FOD on the one hand, and the pulse launched under the combined effects of quintic effect, FOD and IPRS on the other hand. We can see clearly in figure 5a the dispersion of the spectrum but in figure 5b we show that the restoration of the pulse is due to the mutual interaction of the combined effect of the fourth-order dispersion, the quintic effect and intrapulse Raman scattering. One can say that these three effects act together on the pulse to maintain its initial shape.

5. Conclusion

Several techniques and methods are used to reduce the impact of nonlinear effects. Among these techniques or methods are the combination of the three effects cited above. In our numerical simulations, we study the impact of quintic nonlinearity coefficient in the presence of intrapulse Raman scattering and fourth-order dispersion on the appearance of dispersive side-band waves on opposite sides, in the red and blue regions, of the input spectrum. Our results indicate that this difference in power between two peaks tends to disappear with

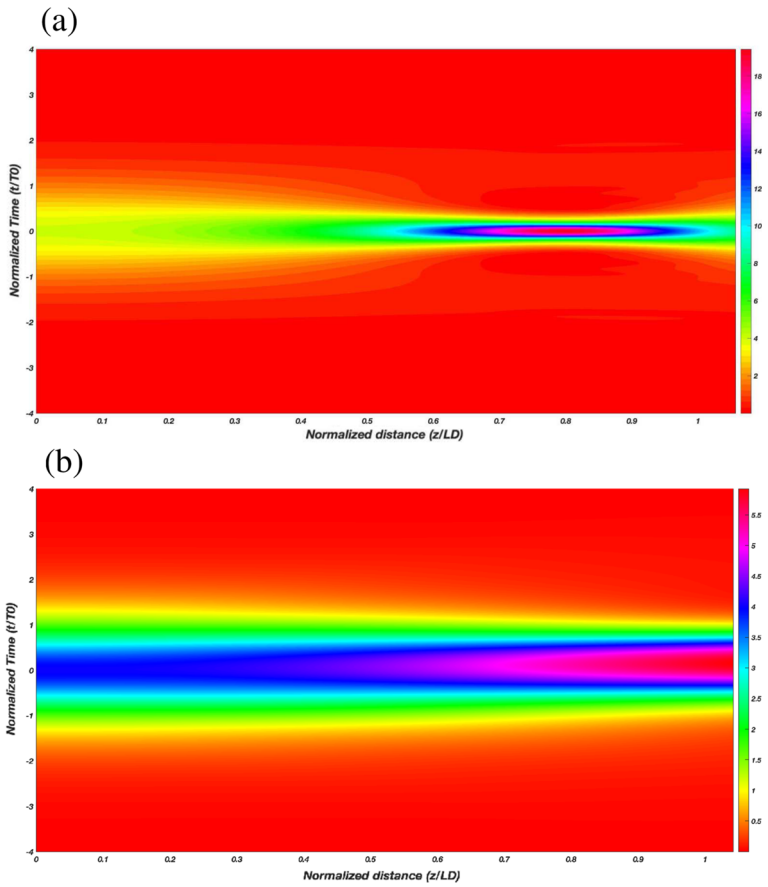

Figure 5. Spectral evolution of higher-order soliton for $z/L_D = 1.06$ in the optical fibre (**a**) when $|\alpha_6| = 0.00$, $\alpha_4 = 0.001$, $|\alpha_8| = 0.00$, $N = 2$, in the presence of only fourth-order dispersion and (**b**) when $|\alpha_6| = 0.10$, $\alpha_4 = 0.001$, $|\alpha_8| = 0.04$, $N = 2$, in the presence of the combination of the three effects, the quintic nonlinearity, FOD and IPRS.

the increase of the value of the quintic nonlinear coefficient. As one may expect, the spectrum tends to the initial triangular shape because of a continuous transfer of energy from these two sideband waves to the main part of the pulse. From the above, it can be concluded that the quintic nonlinear effects can reduce in a considerable way, even eliminate the perturbing effects of Raman scattering and fourth-order dispersion. We can conclude that there is the possibility of stabilisation of higher-order solitons by the compensation of quintic nonlinearity, fourth-order dispersion and Raman process in optical fibres. Finally, these efforts and potentially valuable results await future investigations.

Acknowledgements

This work is in part a contribution to the Post Graduation of Physics and the Physics of Radiations and their Interaction with Matter laboratory (LPRIM), Department of Physics, Faculty of Matter Sciences, University of Batna 1, Hadj Lakhdar, Algeria.

References

[1] G P Agrawal, *Nonlinear fibre optics*, 6th Edn (Academic Press, New York, 2019)
[2] A Hasegawa and Y Kodama, *Solitons in optical communications* (Oxford University Press, Oxford, 1995)
[3] A Hasegawa and M Matsumoto, *Optical solitons in fibres* (Springer, New York, 2002)
[4] S Roy, S K Bhadra and G P Agrawal, *Opt. Commun.* **282**, 3798 (2009)
[5] P K A Wai, C R Menyuk, Y C Lee and H H Chen, *Opt. Lett.* **11**, 464 (1986)
[6] S Roy, S K Bhadra and G P Agrawal, *Opt. Commun.* **283**, 3081 (2010)
[7] K Tai, A Hasegawa and N Bekki, *Opt. Lett.* **13**, 392 (1982)
[8] N Akhmediev and M Karlsson, *Phys. Rev. A* **51**, 2602 (1995)
[9] S Konar, M Mishra and S Jana, *Physica D* **195**, 123 (2004)
[10] J Xu, Y Zheng and X Sun, *16th International Conference on Optical Communications and Networks (ICOCN)* (2017)

[11] A K Shafeeque Ali, K Porsezian and T Uthayakumar, *Phys. Rev. E* **90**, 042910 (2014)
[12] A Hasegawa, *Opt. Lett.* **8**, 650 (1983)
[13] M F Ferreira, *Nonlinear effects in optical fibres* (Wiley-Blackwell, New Jersey, 2011)
[14] M Smadi and D Bahloul, *Comput. Phys. Commun.* **182**, 366 (2011)
[15] M Smadi and D Bahloul, *J. Phys: Conf. Ser.* **574**, 012035 (2015)
[16] S Roy, D Ghosh, S K Bhadra and G P Agrawal, *Phys. Rev. A* **79**, 023834 (2009)
[17] J P Gordan and L F Mollenauer, *Solitons in optical fibres: Fundamentals and applications* (Academic Press, Boston, 2006)
[18] R H Stolen and W J Tomlinson, *J. Opt. Soc. Am. B* **9**, 565 (1992)
[19] A K Shafeeque Ali, M Z Ullah and M Lakshmanan, *Phys. Lett. A* **384**, 126744 (2020)
[20] L J Hua, C Rogers, K W Chow and K S Chiang, *Commun. Theor. Phys.* **61**, 735 (2014)